Understanding the dynamics and complexity of the interstitial drug transport: integration of *in silico* and *in vivo* experiments

Kasia Rejniak
Integrated Mathematical Oncology, Moffitt Cancer Center

Micro & Macro Systems in Life Sciences, June 8-13, 2015

Complexity of tumor microenvironment (TmE)

- ***Stromal cellular structure***
  endothelial cells, fibroblasts, immune cells
- ***Stromal physical structure***
  ECM fiber structure (collagen, elastin, laminin, fibronectin)
- ***Stromal chemical structure***
  growth factors, oxygen, MMPs, metabolites, pH
- ***Stromal fluid structure***
  interstitial fluid flow, interstitial fluid pressure
- ***Host tissue structure***

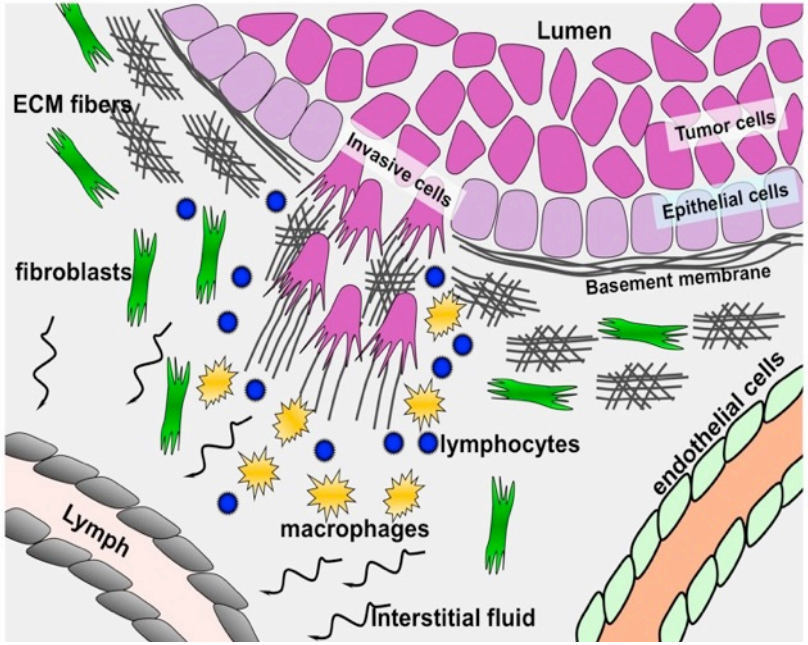

Rejniak & McCawley, *"*Current trends in mathematical modeling of tumor–microenvironment interactions: a survey of tools and applications", ***Exper. Biology & Medicine 2010***

TmE & acquired drug resistance

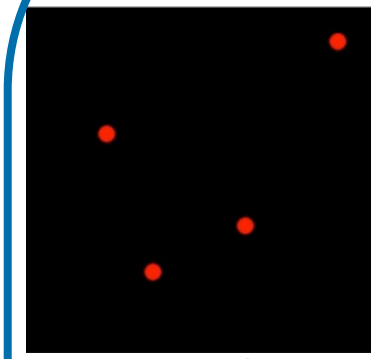
vessels

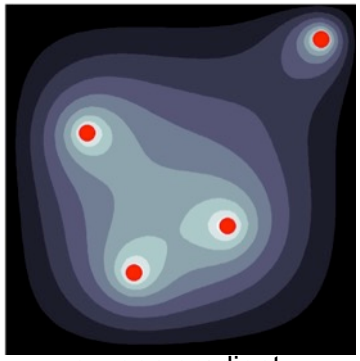
oxygen gradient

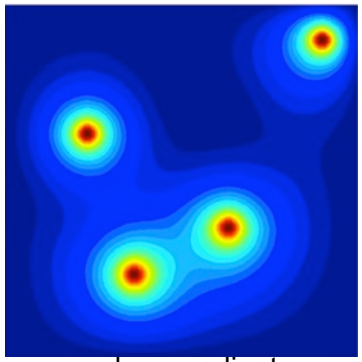
drug gradient

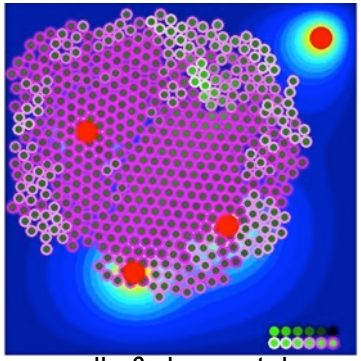
cells & drug uptake

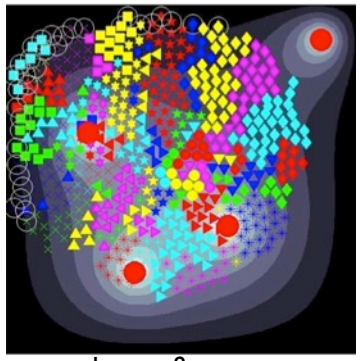
clones & oxygen

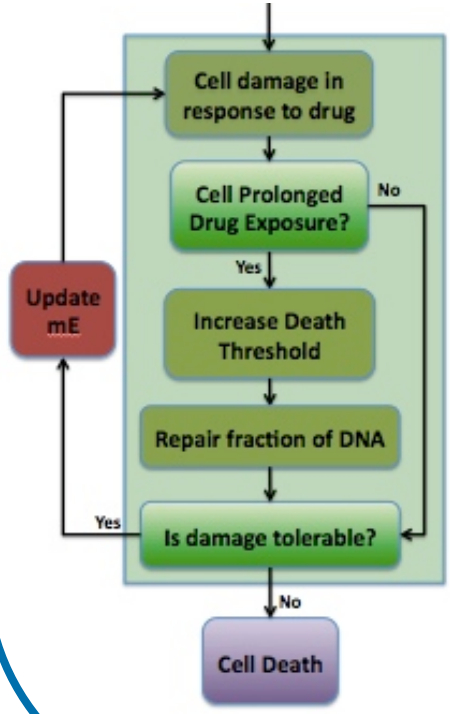

We consider a hypothetical drug damaging DNA:

(i) Cells have some tolerance to DNA damage
(ii) Cells continuously repair damage
(iii) Exposure to drug will induce DNA damage
(iii) High concentration of absorbed drug results in damage that kills the cell
(iv) Prolonged exposure to a low levels of a drug increases cell tolerance

Q: What microenvronmental conditions promote emergence of drug resistance?

IMA WhAM! workshop proceedings
Gevertz, Aminzare, Norton, Perez-Velazquez, Volkening, ***Rejniak****; Springer, July 2015*

TmE niches drive drug resistance

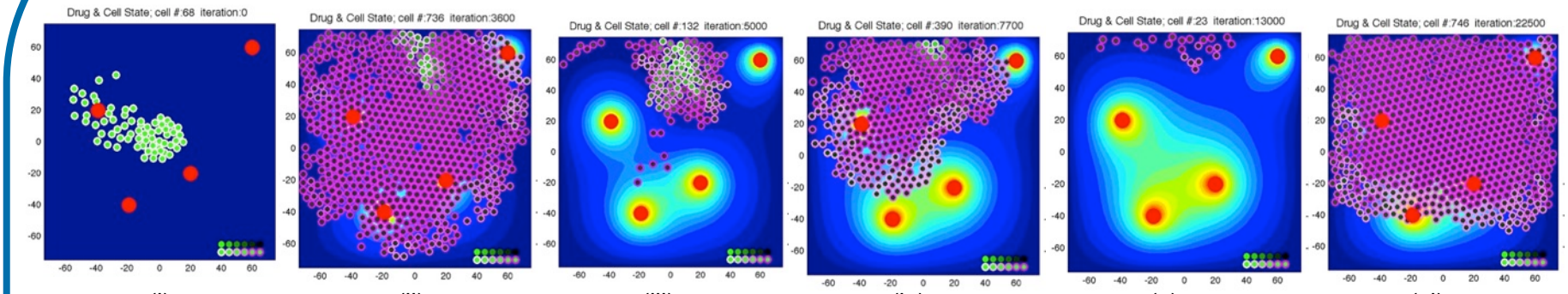

(i) (ii) (iii) (iv) (v) (vi)

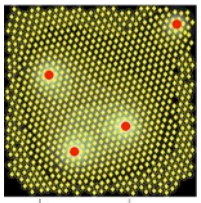

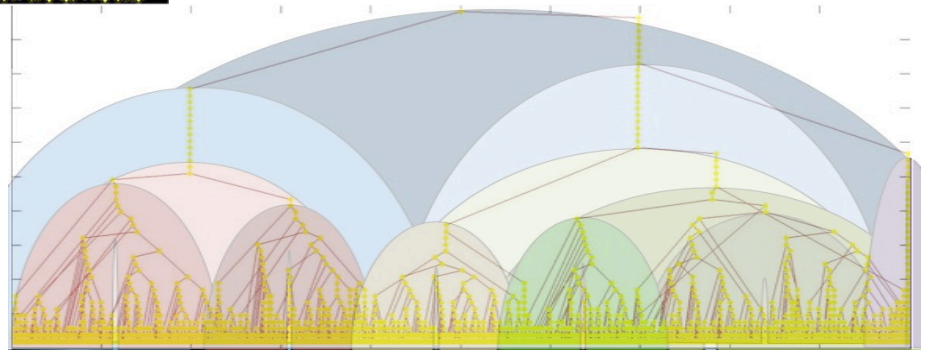

A phylogenetic tree recreated from the survived daughter cells show predecessors that give rise to new subclonesas as a result of their adaptation to microenvironmental niches under the chemotactic treatment.

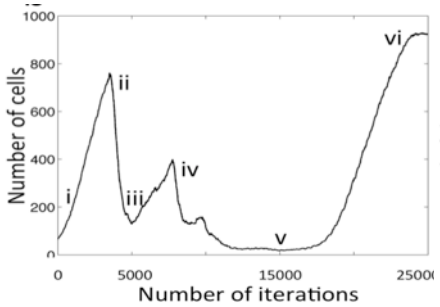

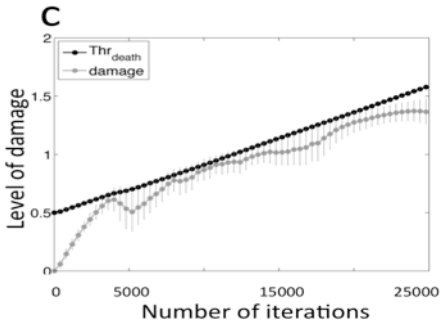

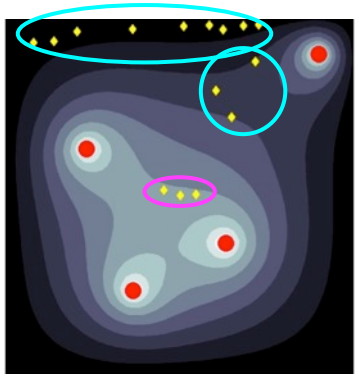

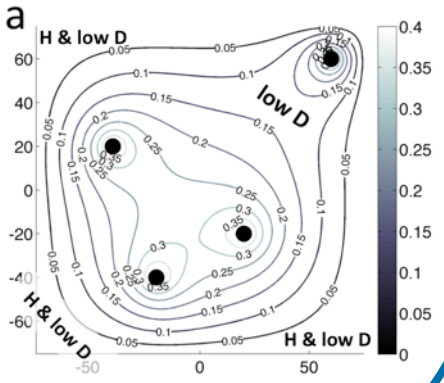

Gevertz, Aminzare, Norton, Perez-Velazquez, Volkening, ***Rejniak****; Springer, July 2015*

Model equations
hybrid; lattice-free

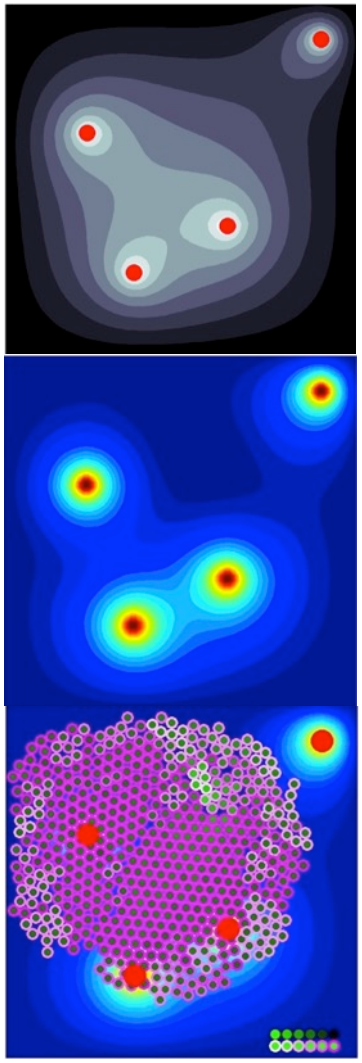

oxygen gradient η
drug gradient γ
cells & drug uptake

$$\frac{\partial \eta(\mathrm{x},t)}{\partial t} = \underbrace{\mathcal{D}_\eta \Delta \eta(\mathrm{x},t)}_{diffusion} - \underbrace{\min\left(\eta(\mathrm{x},t), p_\eta \sum_k \chi C_k^{(X,Y)}(t)\right)}_{uptake\ by\ the\ cells} + \underbrace{S_\eta \sum_j \chi V_j^{(X,Y)}}_{supply}.$$

$$\frac{\partial \gamma(\mathrm{x},t)}{\partial t} = \underbrace{\mathcal{D}_\gamma \Delta \gamma(\mathrm{x},t)}_{diffusion} - \underbrace{d_\gamma \gamma(\mathrm{x},t)}_{decay} - \underbrace{\min\left(\gamma(\mathrm{x},t), p_\gamma \sum_k \chi C_k^{(X,Y)}(t)\right)}_{uptake\ by\ the\ cells} + \underbrace{S_\gamma(t) \sum_j \chi V_j^{(X,Y)}}_{supply}$$

$$\chi C_k^{(X,Y)}(t) = \begin{cases} 1 & \|\mathrm{x} - C_k^{(X,Y)}(t)| < R \\ 0 & \text{otherwise} \end{cases} \qquad \chi V_j^{(X,Y)} = \begin{cases} 1 & \|\mathrm{x} - V_j^{(X,Y)}\| < R_V \\ 0 & \text{otherwise} \end{cases}$$

Cell=($\mathbf{x}_i$(t),R)

$$F_i = -\nu \frac{d\mathbf{x}}{dt}$$

$$\begin{aligned} F_i &= f_{i,j_1} + \ldots + f_{i,j_M} = \\ &= \mathcal{S}\left(d - \|\mathbf{x}_i - \mathbf{x}_{j_1}\|\right) \frac{\mathbf{x}_i - \mathbf{x}_{j_1}}{\|\mathbf{x}_i - \mathbf{x}_{j_1}\|} + \ldots + \mathcal{S}\left(d - \|\mathbf{x}_i - \mathbf{x}_{j_M}\|\right) \frac{\mathbf{x}_i - \mathbf{x}_{j_M}}{\|\mathbf{x}_i - \mathbf{x}_{j_M}\|}. \end{aligned}$$

$$\mathbf{x}_i(t + \Delta t) = \mathbf{x}_i(t) - \frac{1}{\nu} \Delta t F_i$$

Pancreatic cancers TmE

Characteristic of pancreatic Tumor MicroEnvironment (TmE):

- Dense stroma (desmoplasia)
- Stromal cellular and fibrillar components
- Stromal components can outnumber cancer cells
- Increased secretion of collagen by activated myofibroblasts
- Abnormal configuration of blood and lymphatic vessels due to accumulated ECM; hypovascularity & perfusion impairment
- Increased hypoxia (regions of low level of oxygen, <10mmHg)

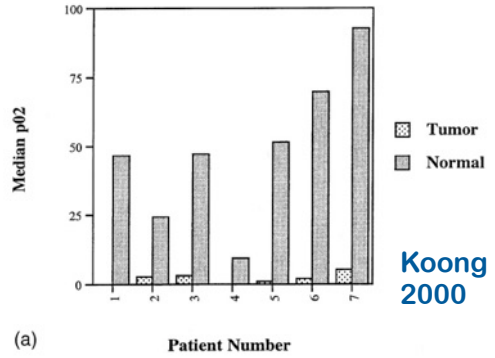

Koong et al. 2000

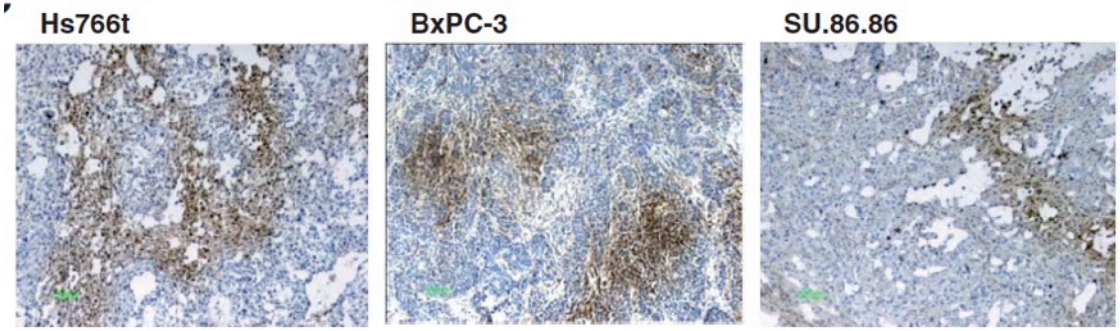

Pimonidazole (PIMO) staining for hypoxia

Sun et al. 2012

Mouse models of PDAC

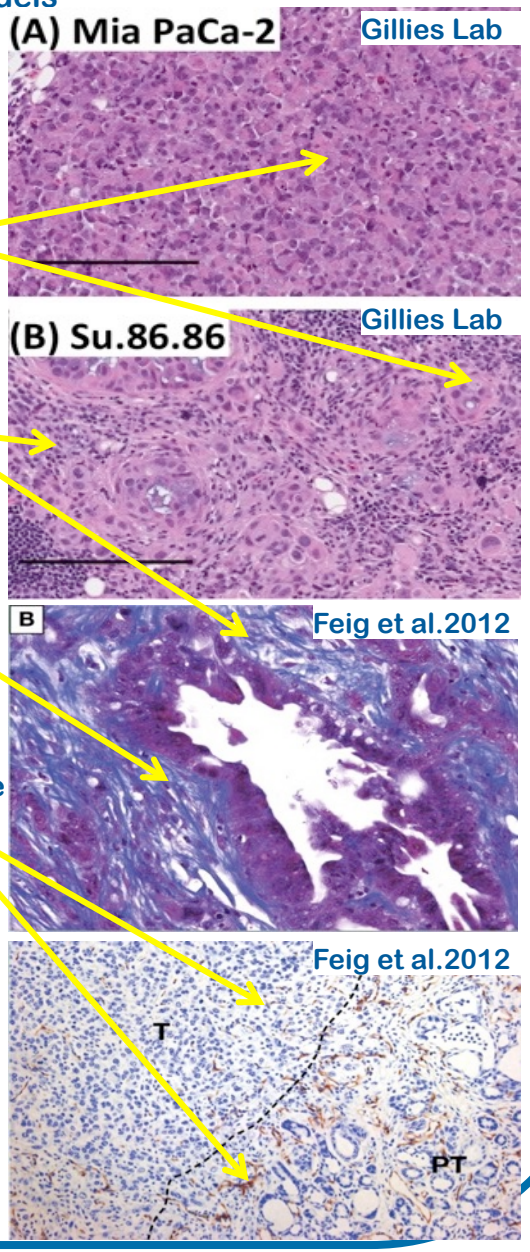

Hypoxia-activated drugs

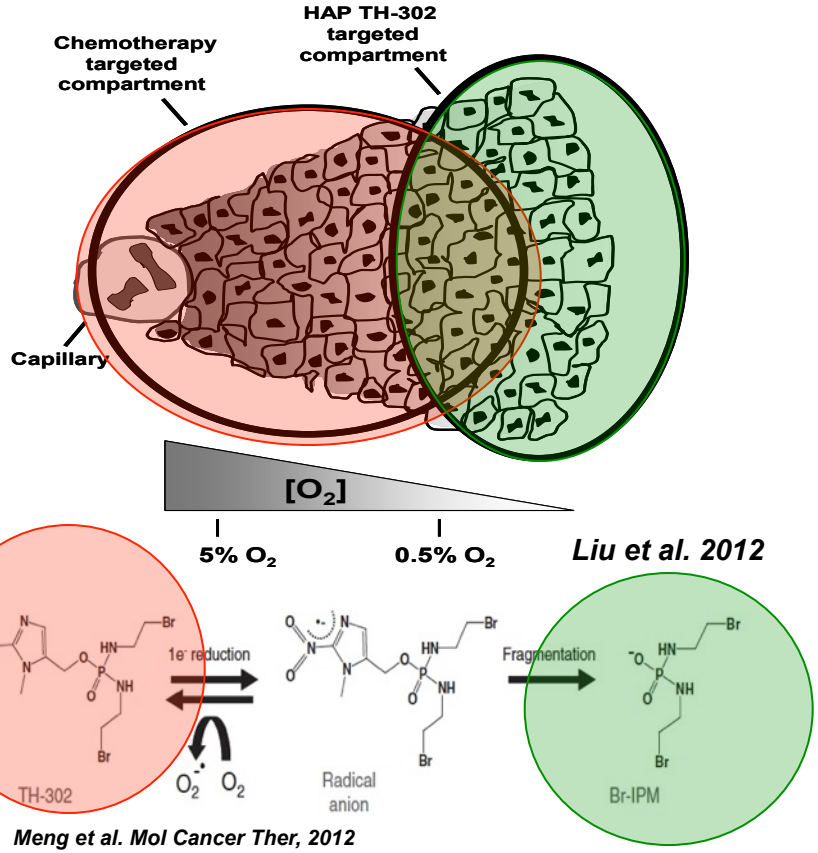

Meng et al. Mol Cancer Ther, 2012

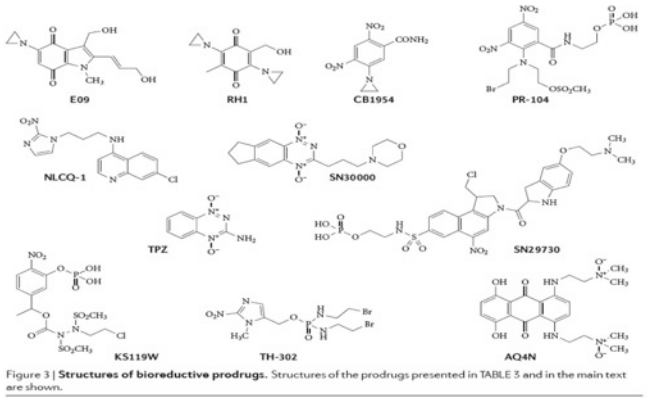

Figure 3 | **Structures of bioreductive prodrugs.** Structures of the prodrugs presented in TABLE 3 and in the main text are shown.

Wilson, Hay, Nature Rev. Cancer, 2011

- ***Mechanisms of HAP action:***
- ***Enters tumor tissue from the vasculature as an bioreductive (inactive) pro-drug***
- ***Inactive when O_2 level above 10mmHg***
- ***Chemical activation in low oxygen levels (below 10mmHg)***
- ***Lethal effect on cells upon accumulation (DNA crosslink or damage)***
- ***Relatively short plasma half-life***

In silico tissue morphology & tissue oxygenation

MiaPaCa-2
Human pancreatic carcinoma cell line

J. Wojtkowiak, R. Gillies Lab

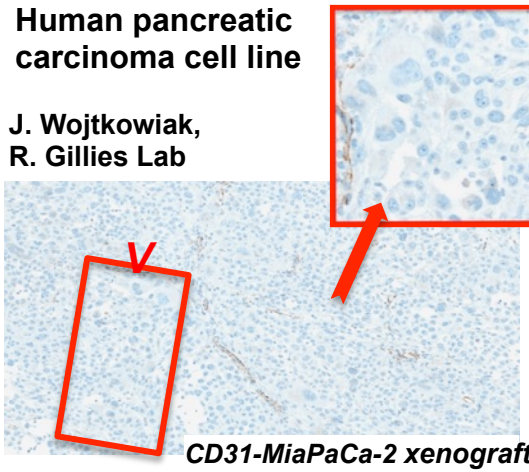

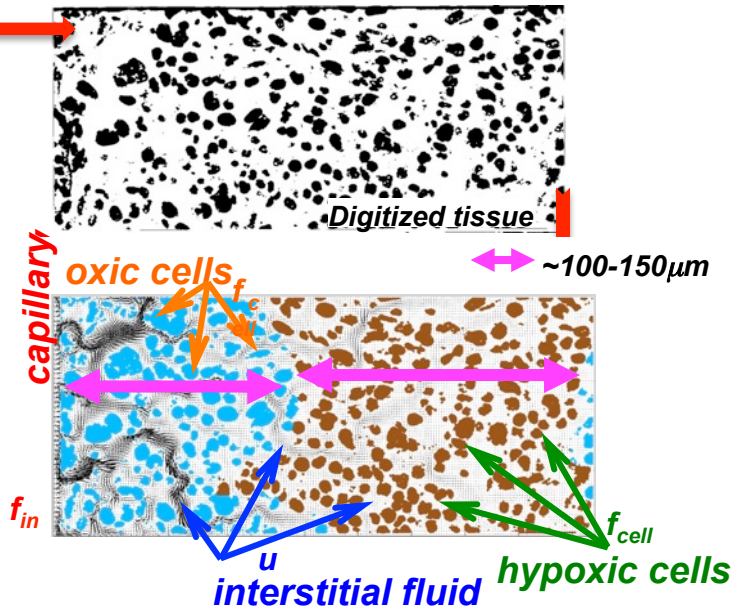

Tissue oxygenation: balance between O_2 influx, diffusion and cellular consumption:

- O_2 level in the blood: 60mmHg
- O_2 diffusion: $10^{-6}cm^2/s$
- Hypoxia: <10mmHg
- IF velocity: <2μm/s
- Cell consumption fitted to reach hypoxia at 100-120μm from vasculature

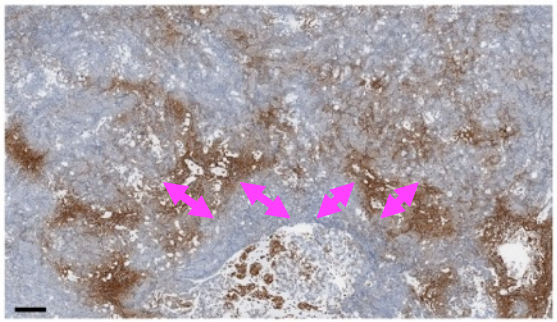

J. Wojtkowiak, R. Gillies Lab

MiaPaCa-2, pimonidazole staining

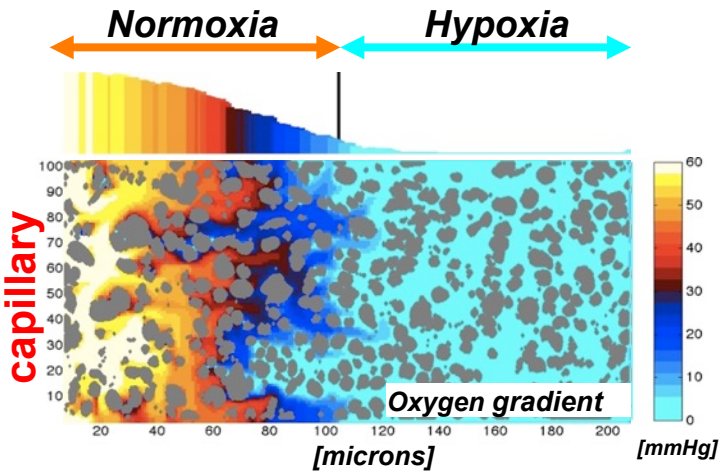

HAPs action – microPD model

Mathematical model:

Regularized Stokeslets (1)-(2)
Diffusion: O_2 (*c*), inactive HAP (η_i), active HAP (η_a)
Advection: interstitial fluid (**u**)
Activation: pro-drug
Uptake: O_2 (*MM*), active HAP (*absorb*)
Lethal effect: active HAP

$$\mu\Delta\mathbf{u}(\mathbf{x}) = \nabla p(\mathbf{x}) - \mathbf{f}(\mathbf{x}) \quad \text{and} \quad \nabla\cdot\mathbf{u}(\mathbf{x}) = 0 \tag{1}$$

$$\text{where} \quad \mathbf{f}(\mathbf{x}) = \mathrm{f}_0\,\phi_\varepsilon(\mathbf{x}-\mathbf{x}_0), \quad \text{and} \quad \phi_\varepsilon(\mathbf{x}) = \frac{2\varepsilon^4}{\pi(\|\mathbf{x}\|^2+\varepsilon^2)} \tag{2}$$

$$\frac{\partial c(\mathbf{x},t)}{\partial t} = \underbrace{\mathcal{D}_c\Delta c(\mathbf{x},t)}_{diffusion} - \underbrace{\mathbf{u}(\mathbf{x},t)\cdot\nabla c(\mathbf{x},c)}_{advection} - \underbrace{\frac{\kappa_m c(\mathbf{x},t)}{\kappa_n + c(\mathbf{x},t)}\chi(\Omega_\Gamma)}_{cellular\ \ uptake} \tag{3}$$

$$\frac{\partial \eta_i(\mathbf{x},t)}{\partial t} = \underbrace{\mathcal{D}_{\eta_i}\Delta\eta_i(\mathbf{x},t)}_{diffusion} - \underbrace{\mathbf{u}(\mathbf{x},t)\cdot\nabla\eta_i(\mathbf{x},c)}_{advection} - \underbrace{\xi(c(\mathbf{x},t))\eta_i(\mathbf{x},t)}_{activation} - \underbrace{\omega_i\eta_i(\mathbf{x},t)}_{decay} \tag{4}$$

$$\frac{\partial \eta_a(\mathbf{x},t)}{\partial t} = \underbrace{\mathcal{D}_{\eta_a}\Delta\eta_a(\mathbf{x},t)}_{diffusion} - \underbrace{\mathbf{u}(\mathbf{x},t)\cdot\nabla\eta_a(\mathbf{x},c)}_{advection} + \underbrace{\xi(c(\mathbf{x},t))\eta_i(\mathbf{x},t)}_{activation} - \underbrace{\alpha\eta_a(\mathbf{x},t)\chi(\Omega_\Gamma)}_{cellular\ \ uptake} \tag{5}$$

$$\text{initial conditions:} \quad \mathbf{u}(\mathbf{x},t_0) = \mathbf{u_0}(\mathbf{x}), \quad c(\mathbf{x},t_0) = c_0(\mathbf{x}),$$
$$\text{vessel boundary conditions:} \quad \mathbf{u}(\mathbf{x_0},t) = \mathbf{u^0}, \ c(\mathbf{x_0},t) = c^0, \ \eta_i(\mathbf{x_0},t) = \eta_i^0.$$

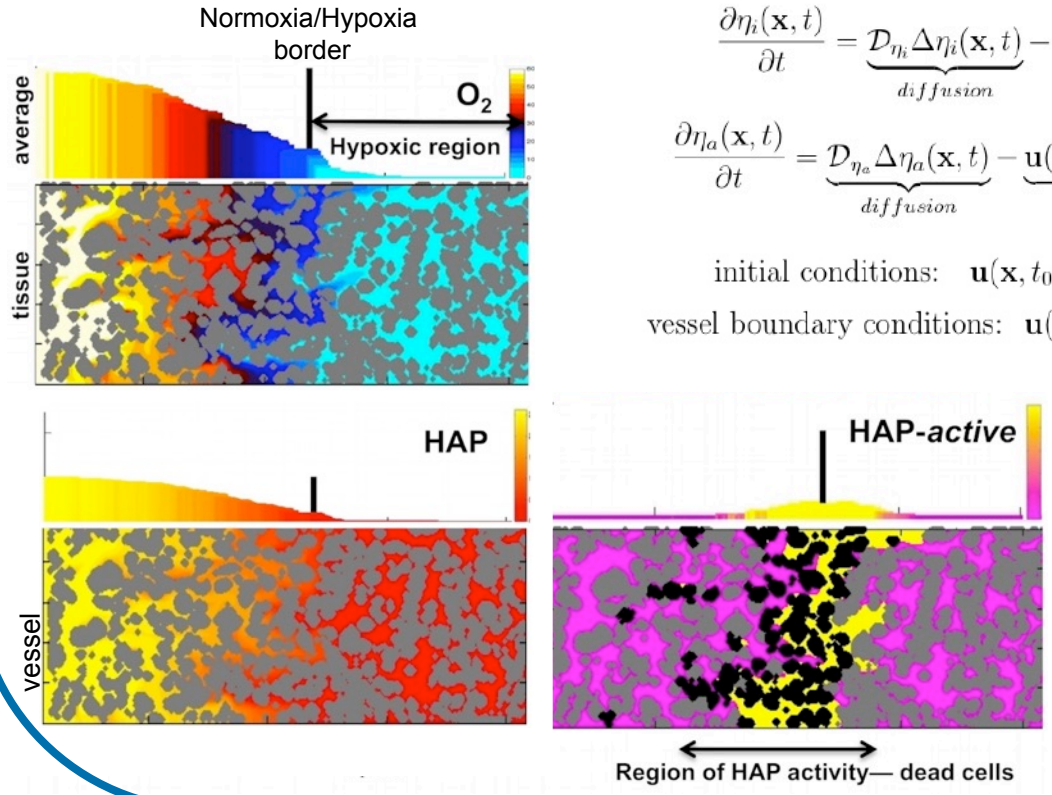

Wojtkowiak et al. Cancer & Metabolism 2015

HAPs-O_2 interplay

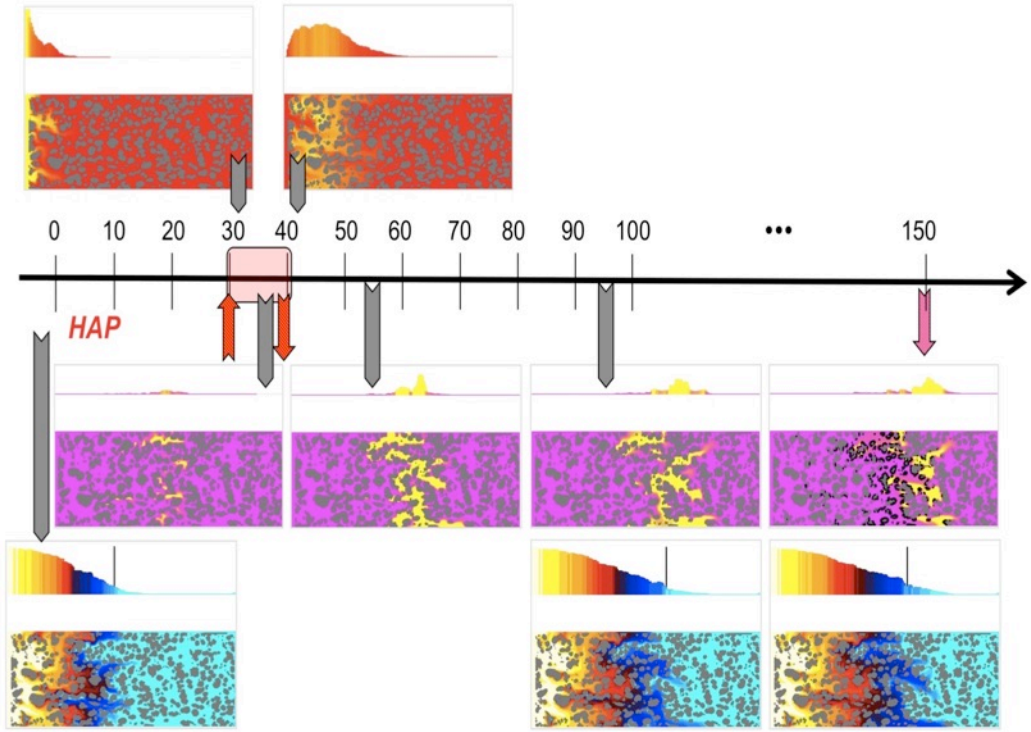

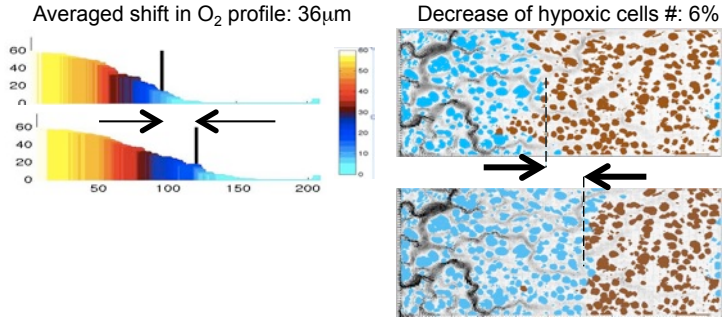

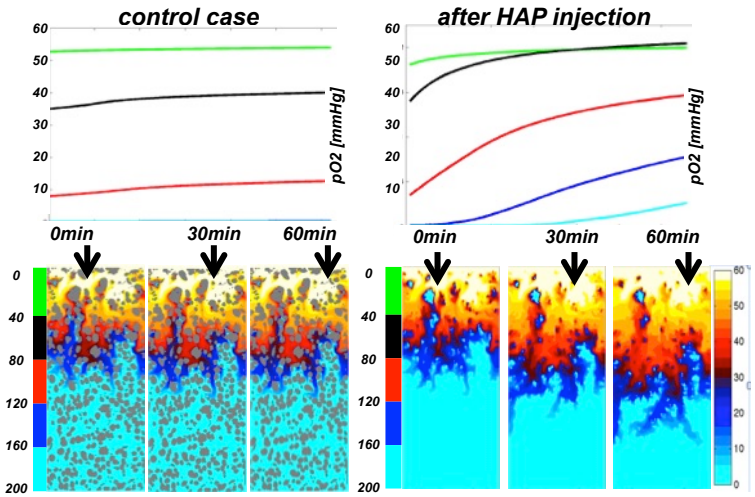

HAP injection can perturb the metabolic landscape of a tissue and increase the O_2 levels due to diminished oxygen uptake as a result of cell death. The steady gradient of O_2 (control case) can be shifted after HAP application.

- Bolus injection
- HAP dosage: 50mg/kg
- HAP max plasma concentration: ~40μg/ml
- HAP systemic clearance ~ 10min
- HAP (inactive) diffusion ~ O_2 diffusion
- HAP (active) diffusion ~ 2*HAP inactive

Duan et al.2008; Jung et al. 2012;

Time-course analysis of oxygen contents in five tissue zones (color-coded green-to-cyan) at three specific time points.

Efficacy of hypoxia-activated drugs

efficacy of interstitial space penetration

=

vascular influx + *extracellular transport* + *cellular uptake*

Enhancing HAP efficacy vasodilators

efficacy of interstitial space penetration
=
vascular influx + ***extracellular transport*** + ***cellular uptake***

decreasing O_2 influx

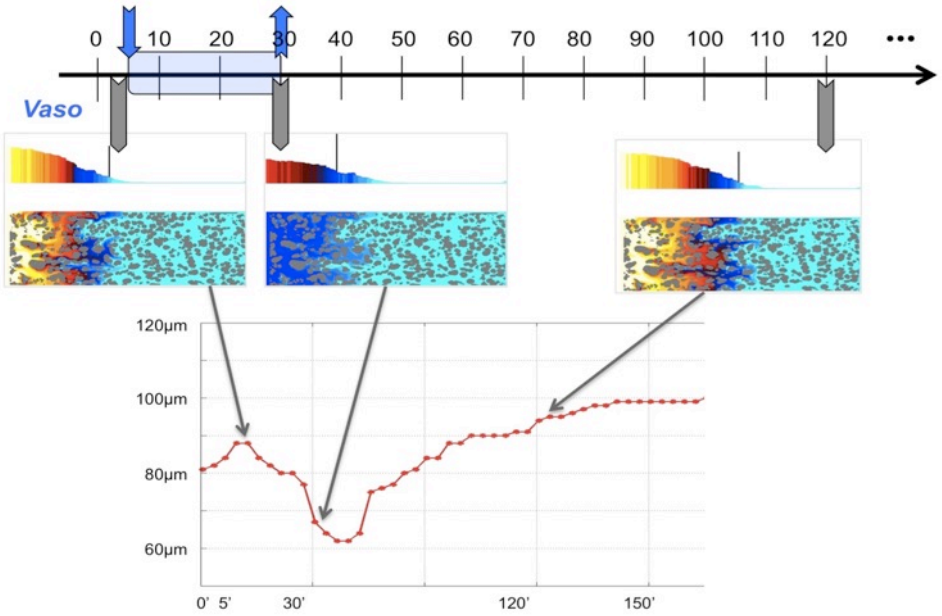

Change of boundary conditions:
Vascular influx of water and oxygen reduced in half

Vasodilator:
- Bolus injection
- Diminished influx of water
- Diminished influx of O_2
- Kinetics fitted to reduce oxygen content according to experimentally reported values
- Kinetics fitted such that O_2 returns to normal levels according to experimentally reported time

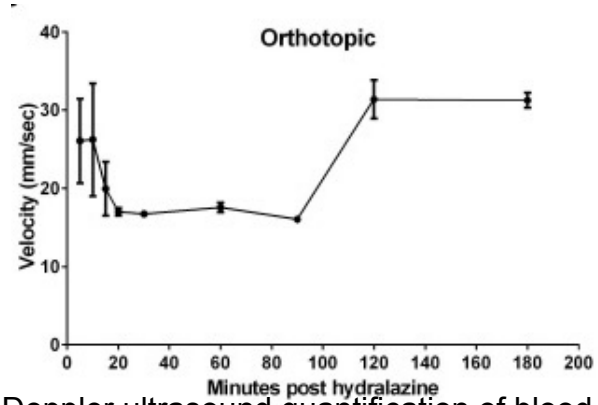

Doppler ultrasound quantification of blood flow

R. Gillies lab, Moffitt

Steal phenomena

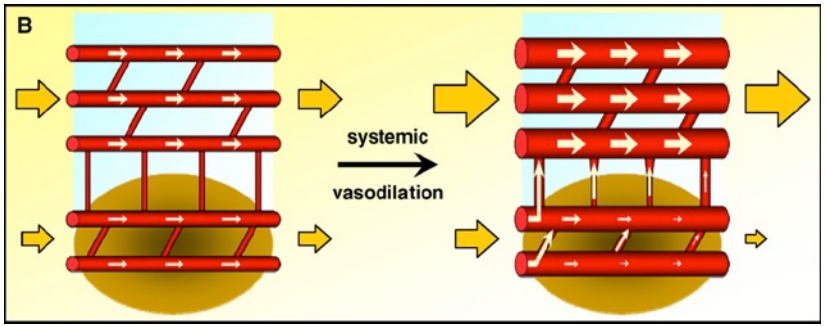

"steal phenomena"*:* vasodilators cause normal vessels to dilate resulting in a systemic drop in blood pressure that reduces tumor perfusion as the blood is diverted from the tumor vascular bed (vascular steal).

Sonveaux, 2008

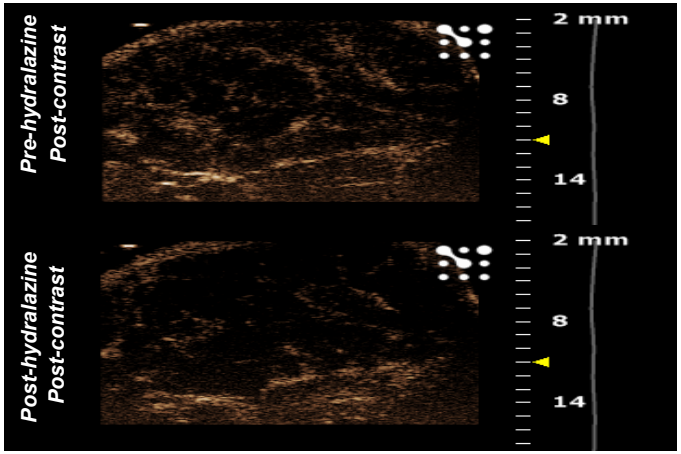

Contrast Enhanced Ultrasound.
Ultrasound contrast agent (micro-bubbles) shows vascular space in a mouse with MiaPaca-2 tumor: ***Top****: pre-treated;* ***Bottom:*** *hydralazine-treated (30 min after injection) showing 31% decrease in the amount of contrast agent being delivered within the tumor vasculature.*

MIA PaCa-2: (orthotopic)
reduction in blood flow within 15 min of hydralazine injection,
reduced to minimal levels by 30 minutes,
recovery occurring between 90 and 120 minutes.

SU.86.86 (TH-302 resistant) tumors are well vascularized with mature vessels that would be expected to dilate in response to hydralazine treatment.

MIA PaCa-2 (moderate TH-302 resistance) vasculature is immature and atonal; MIA PaCa-2 tumors exhibit the ‘‘steal’’ effect due to immature tumor vasculature.

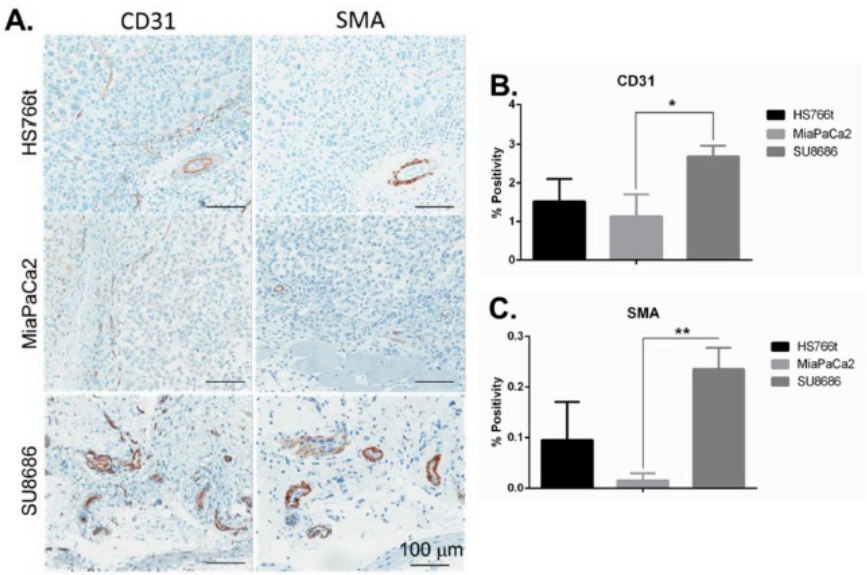

R. Gillies lab, Moffitt

HAP + vasodilator

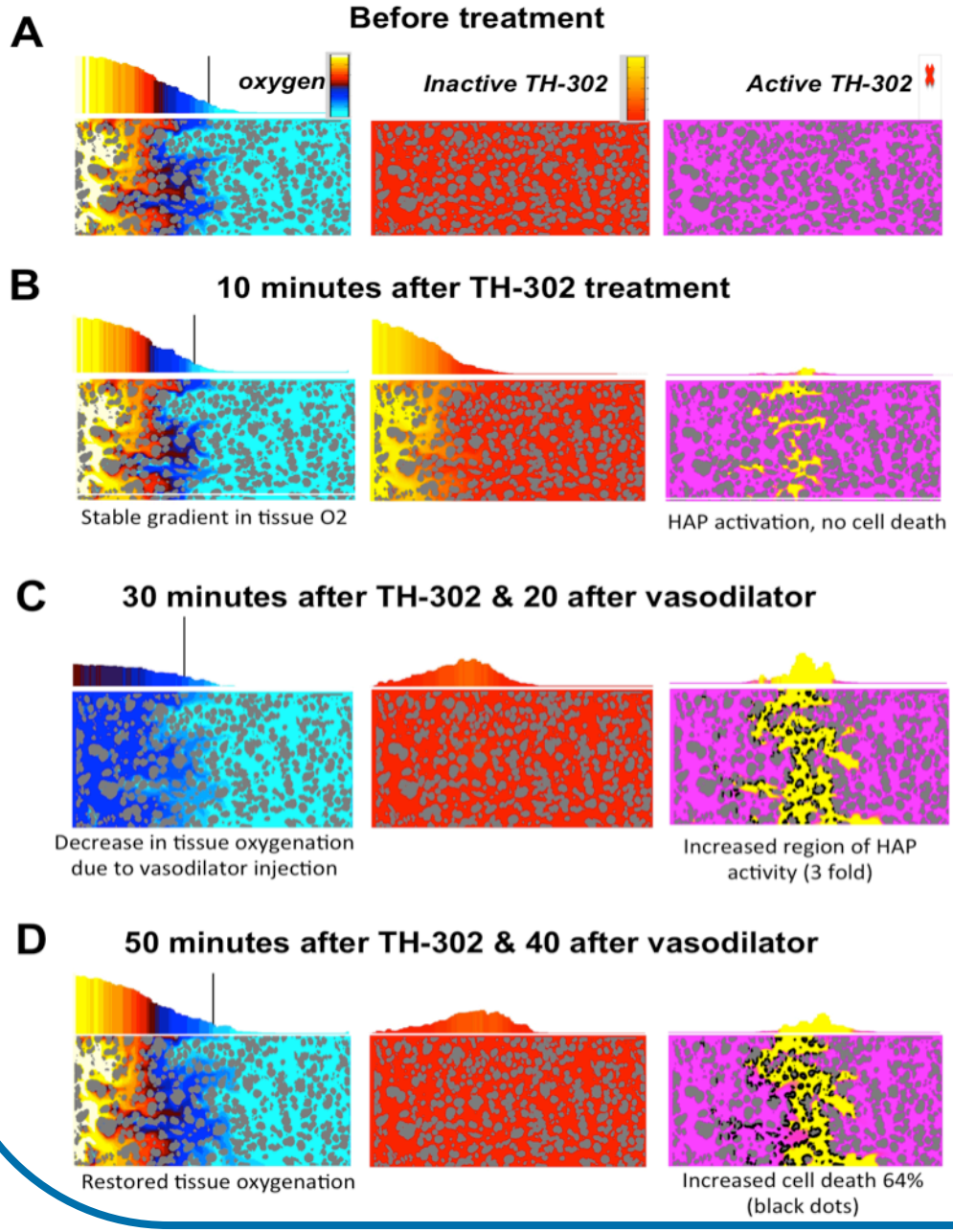

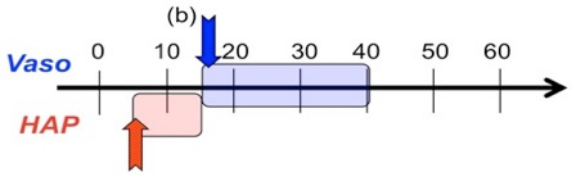

(A) Initial distribution of oxygen before treatment, both inactive and active TH-302 are all absent;

(B) 10 minutes after TH-32 injection;

(C) When a vasodilator is applied, tissue oxygen level is decreased due to limited influx of O2 from the vasculature; the region of HAP activation is enlarged 3-fold;

(D) increased cell death (50% rise after 50 min, when compared to TH-302 injection only.

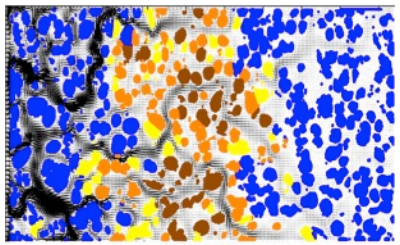

~10% cells

Enhancing HAP efficacy sensitizers

efficacy of interstitial space penetration
=

vascular influx + *extracellular transport* + ***cellular uptake***

increasing O_2 uptake

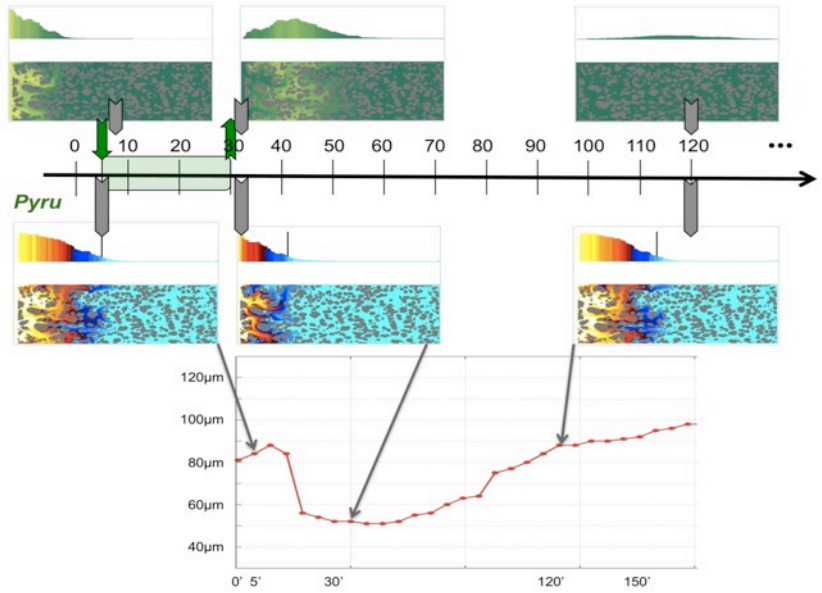

Adding a new equation for pyruvate γ :

$$\frac{\partial \gamma_*(\mathbf{x},t)}{\partial t} = \underbrace{\mathcal{D}_{\gamma_*}\Delta\gamma_*(\mathbf{x},t)}_{diffusion} - \underbrace{\mathbf{u}(\mathbf{x},t)\cdot\nabla\gamma_*(\mathbf{x},c)}_{advection} - \underbrace{\beta\gamma_*(\mathbf{x},t)\chi(\Omega_\Gamma)}_{cellular\ uptake} - \underbrace{\omega_{\gamma_*}\gamma_*(\mathbf{x},t)}_{decay}$$

and for cell response: $\beta = N\beta_0$ if $\gamma_*(\xi,\tau) > \gamma_{\tau\eta\rho}$

Pyruvate:

- Bolus injection
- Diffusion: ~10^{-7}cm^2/s
- Cellular uptake fitted to reach proper increase in O_2 uptake
- Cellular metabolism fitted to return to normal levels in 2 hrs

MiaPaca

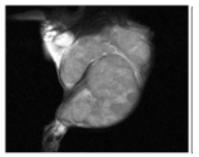

Increased hypoxia fraction in vivo

Pre ***10 min*** ***30 min***

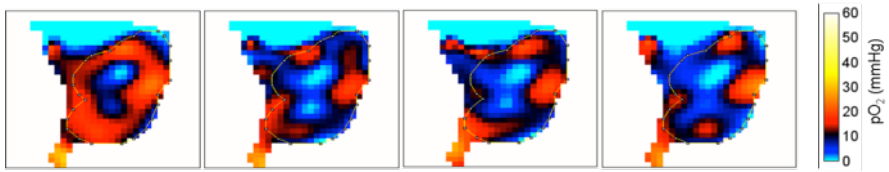

EPR Imaging of increased hypoxic fractions in pancreatic tumor xenografts peak: @ 30min; return to normal levels: five hrs post injection of pyruvic acid

S. Matsumoto, M.C. Krishna lab, NIH

Metabolic sensitizers - pyruvate

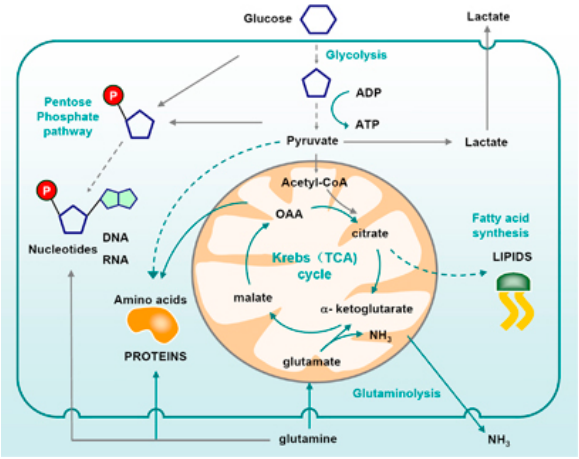

Metabolism of proliferating cells.

Increased oxygen consumption rate in vitro

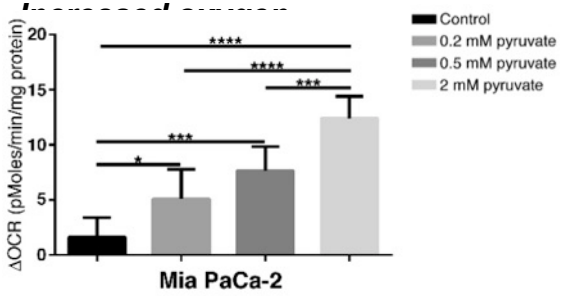

J. Wojtkowiak, R. Gillies lab, Moffitt

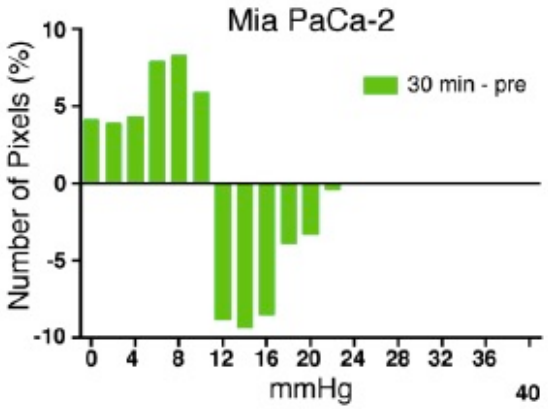

Tumor oxygenation (30 min post pyruvate minus baseline) displayed as percent pixel per pO2 (mmHg).

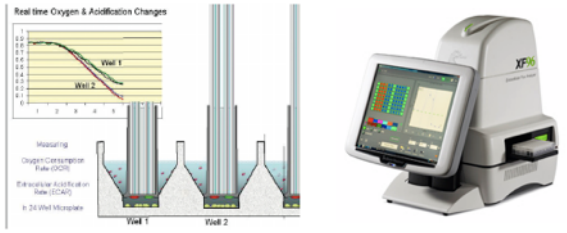

The Seahorse XF96 instrument measures the rate of change of oxygen and pH in the media surrounding living cells cultured in a microplate using fluorescent biosensors in a real-time non-invasive manner.

HAP + pyruvate

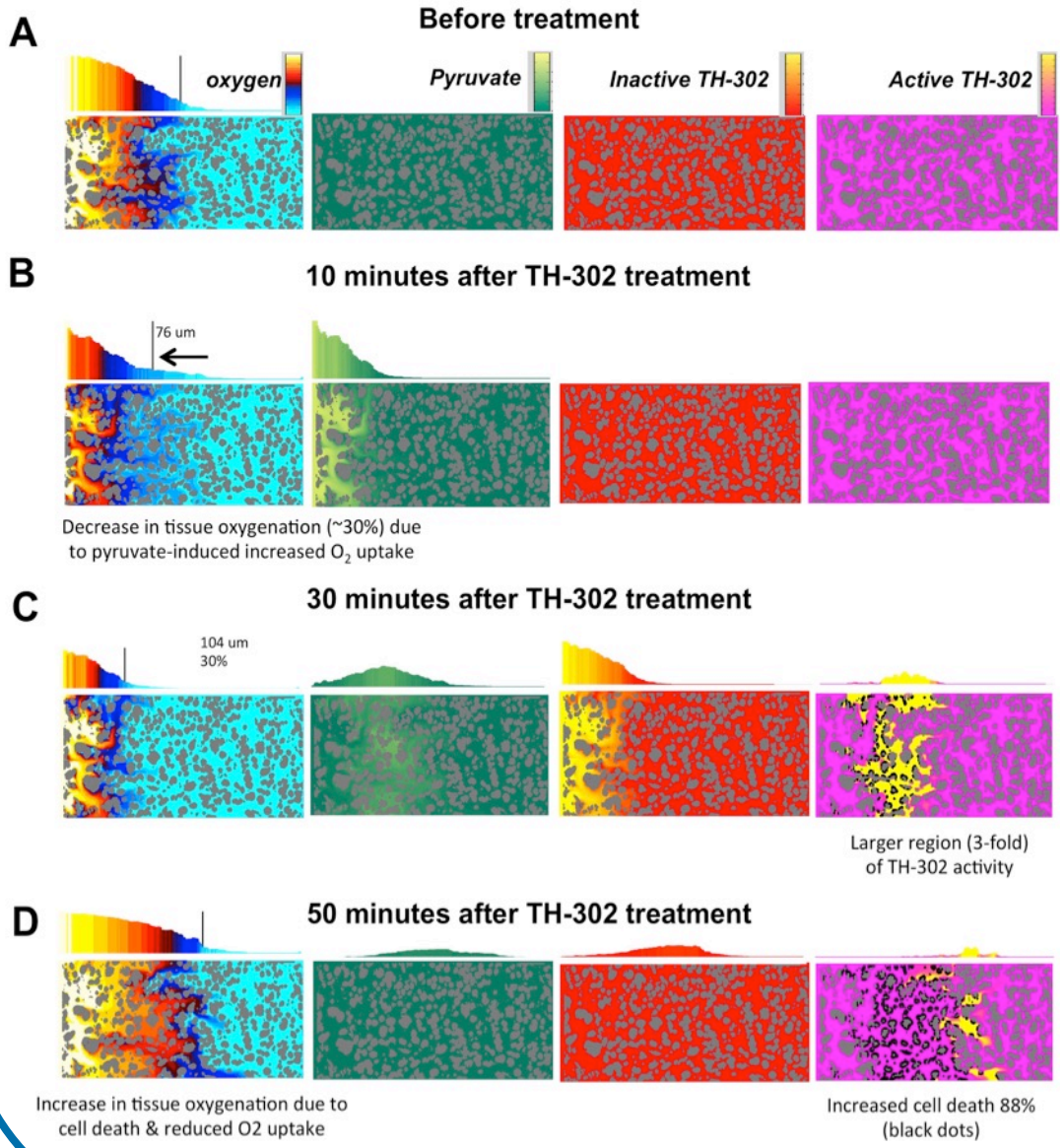

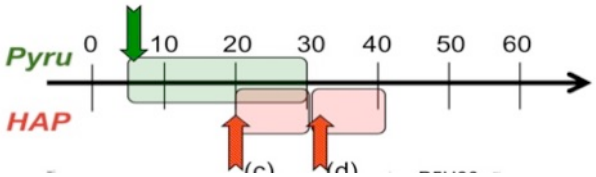

(A) Initial distribution of oxygen before treatment; pyruvate, inactive and active TH-302 are all absent;

(B) When pyruvate is applied before TH-302, tissue oxygen extent is diminished (~30%) due to increased cellular consumption;

(C) The region of HAP activation is enlarged (3-fold) in 10 min after TH-302 injection

(D) Increased cell death (88%) after 50 min from TH-302 injection, when compared to TH-302 only

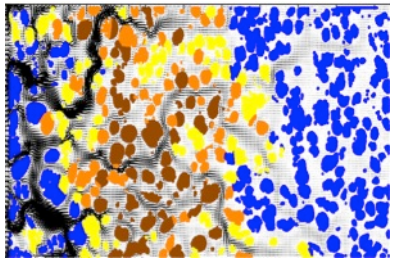

~13%

Enhancing HAP efficacy
Diffusion & half-life

efficacy of interstitial space penetration
=
vascular influx + ***extracellular transport*** + *cellular uptake*

Change in diffusion D2

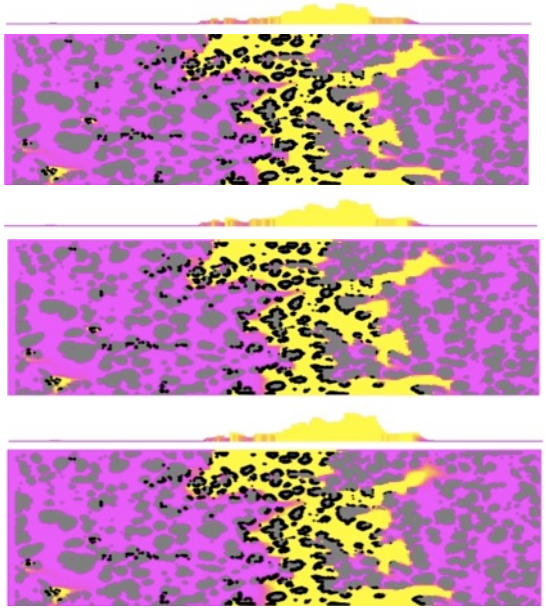

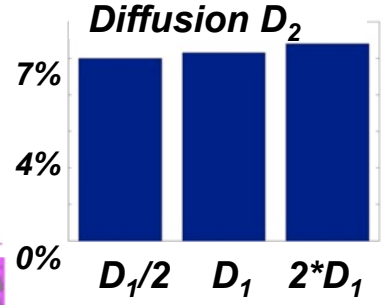

Change in half-life

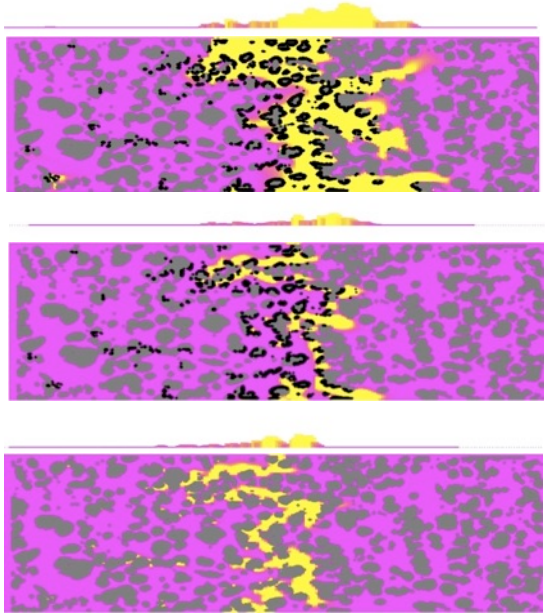

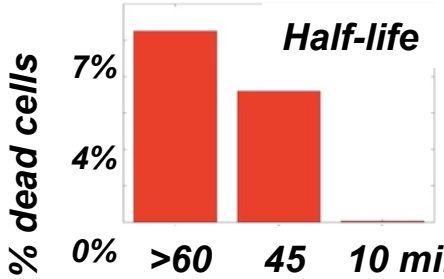

Modifications in drug diffusion (mass) has less impact on the extent of tumor cells death than the active drug half-life

Enhancing HAPs efficacy by combination therapy scheduling

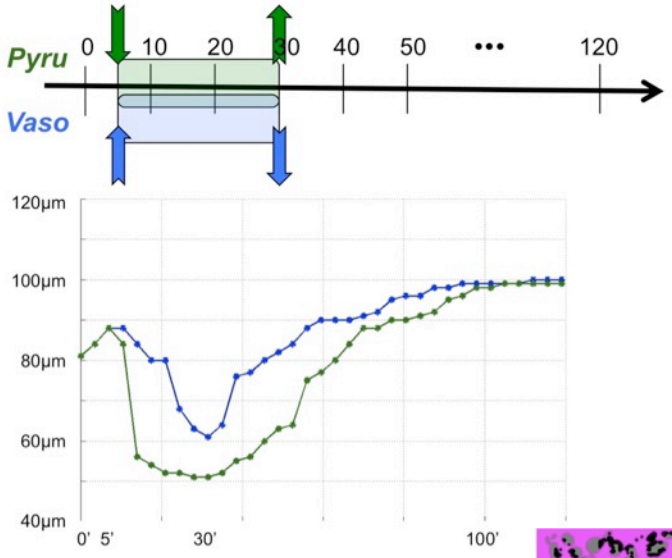

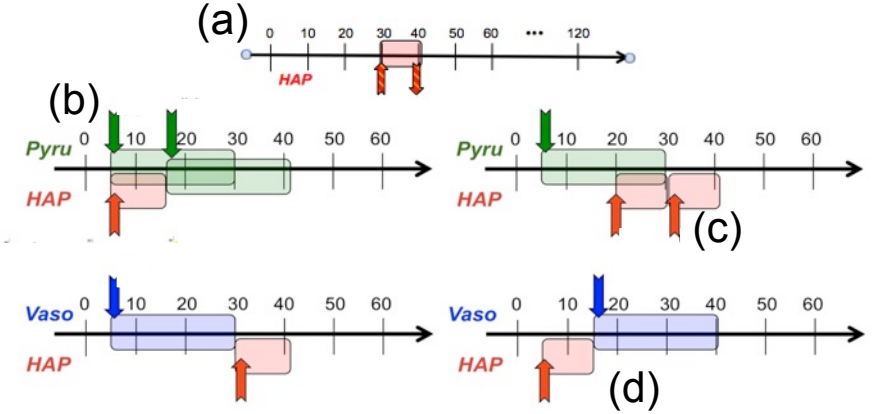

(a) 7%

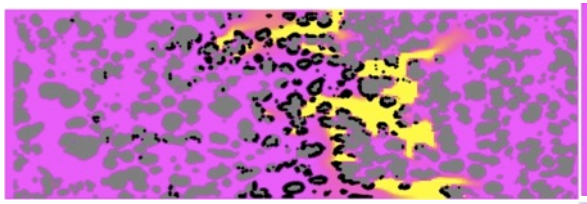

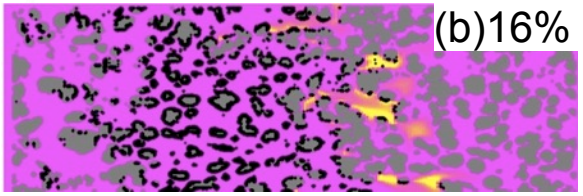

(b)16%

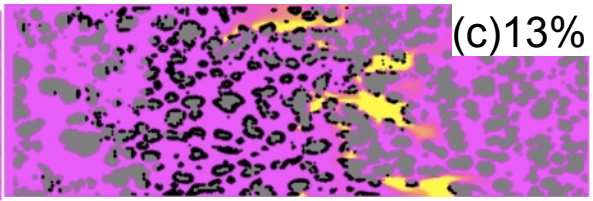

(c)13%

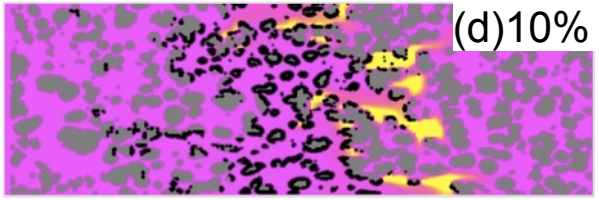

(d)10%

In-vivo effect of pyruvate pre-treatment 30 min prior to HAP administration

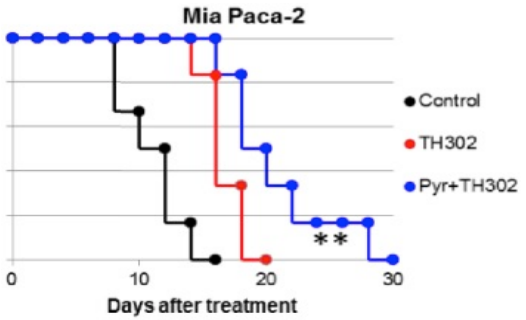

J. Wojtkowiak, R. Gillies lab, Moffitt

Conclusions

- *Hypoxic niches can promote drug-induced drug resistance*
- *Patterns of either advection- or diffusion-dominated interstitial transport depend on tissue architecture for the moderate Peclet #s,*
- *HAPs alone can lead to a shift in tissue metabolic landscape,*
- *The best short-time response is observed when PDAC are sensitized with pyruvate administered together with HAPs,*
- *Modifications of HAPs kinetic properties is not as effective as modulation of tumor microenvironment.*

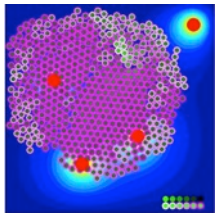

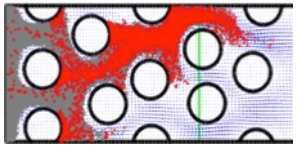

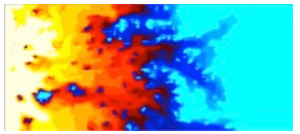

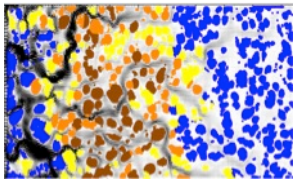

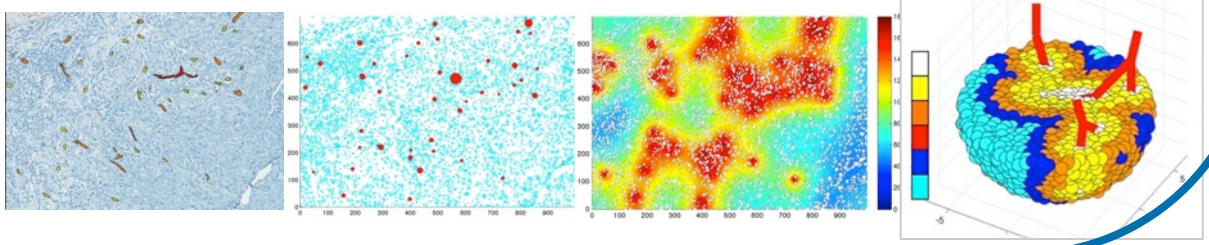

Acknowledgment

IMO, Moffitt
MunJu Kim
Banu Baydil
Tedman Torres

Imaging & Metabolism, Moffitt
Robert Gillies
Dave Morse
Jonathan Wojtkowiak
Veronica Estrella
Heather Cornnell
Allison Cohen

Threshold Pharm.
Charles Hart

Microscopy, Moffitt
Mark Lloyd
Aga Kasprzak
Tingan Chen

Center for Cancer Research, NIH
Shingo Matsumoto
Murali C. Krishna

Contact:
Kasia.Rejniak@moffitt.org
http://labpages.moffitt.org/rejniakk